

**Pseudorandom binary injection of levitons for electron quantum optics**

D. C. Glattli and P. Roulleau

*Service de Physique de l'État Condensé (CNRS UMR 3680), IRAMIS, CEA-Saclay, F-91191 Gif-Sur-Yvette, France*

(Received 20 December 2017; revised manuscript received 16 February 2018; published 8 March 2018)

The recent realization of single-electron sources lets us envision performing electron quantum optics experiments, where electrons can be viewed as flying qubits propagating in a ballistic conductor. To date, all electron sources operate in a periodic electron injection mode, leading to energy spectrum singularities in various physical observables which sometimes hide the bare nature of physical effects. To go beyond this, we propose a spread-spectrum approach where electron flying qubits are injected in a nonperiodic manner following a pseudorandom binary bit pattern. Extending the Floquet scattering theory approach from periodic to spread-spectrum drive, the shot noise of pseudorandom binary sequences of single-electron injection can be calculated for leviton and nonleviton sources. Our new approach allows us to disentangle the physics of the manipulated excitations from that of the injection protocol. In particular, the spread-spectrum approach is shown to provide better knowledge of electronic Hong-Ou-Mandel correlations and to clarify the nature of the pulse train coherence and the role of the dynamical orthogonality catastrophe for noninteger charge injection.

DOI: [10.1103/PhysRevB.97.125407](https://doi.org/10.1103/PhysRevB.97.125407)**I. INTRODUCTION**

The goal of electron quantum optics is to perform with electrons quantum operations similar to those done with photons in quantum optics. Here we consider ballistic quantum conductors where electrons can propagate with no backscattering along electronic quantum modes in a way similar to photons propagating along electromagnetic modes. Many tools commonly encountered in optics are already available in ballistic quantum conductors. The analog of photon beam splitters is obtained with electron beam splitters using quantum point contacts (QPC) which form a local artificial scatterer partitioning a single electron propagating on a single quantum channel into transmitted and reflected channels. Combining two QPC beam splitters in series provides electron analogs of optical Mach-Zehnder [1,2] and Fabry-Pérot interferometers. Such interferometers have been useful to evidence electronic interference and to quantify the degree of coherence of electronic wave packets in the quantum conductor. To go further in the electron-photon analogy, a full electron quantum optics requires the analog of a single-photon source. One appealing perspective is that the time control of single electrons lets us envisage their use as flying qubits [3,4], where the information is encoded in the presence or absence of an electron in a quantum channel or encoded in the spin of the itinerant electron (to mimic photonic flying qubits encoded in the photon polarization). Several approaches have been used to realize the on-demand coherent injection of single electrons [5–11]. Here we consider the voltage pulse source [11,12], which is simpler to build and operate. It is based on voltage pulses applied on a contact to inject a single charge in the ballistic conductor. It was theoretically and experimentally shown that for voltage pulses having a Lorentzian time variation, electrons are injected in the form of a remarkable *minimal excitation state* [13–17], which has been called a *leviton* [11]. Synchronizing the injection of single electrons from different sources [18,19] and letting them

interfere in a quantum conductor let us envisage flying-qubit operation in a simple way. This approach has already led to new quantum experiments where single-electron partitioning [11,20], electronic Hong-Ou-Mandel interference [11,21], and single-electron quantum tomography [12] have been shown.

For practical ease of operation and calculation, only periodic electron injections have been considered to date. However, periodic driving is not mandatory. What is usually needed is a large number of single-electron injections to perform with high enough accuracy the statistical measurements giving the average value of the current or of its fluctuations (current noise) when performing Hong-Ou-Mandel correlations or quantum state tomography. Periodic driving leads to a peculiar dependence in the observables studied. For example, the electron injection at frequency  $\nu = 1/T$  introduces stepwise discontinuities in the electron energy distribution of levitons that are also imprinted on their electronic Wigner function [12,22,23] at energies of multiple  $h\nu$  [24]. These discontinuities manifest through singularities in the shot noise of electrons partitioned by a QPC. They may prevent us from understanding if some observed phenomenon results from periodicity or from the nature of the injected charge. This is unfortunate as understanding the nature of the single-electron state when many electrons are injected is a key issue and a theoretical challenge [25,26]. The ideal situation would be to inject just a single electron and look at the result. This is, however, impossible due to the present lack of reliable single-electron detectors.

We consider here the nonperiodic injection of electrons following a pseudorandom binary bit pattern  $\{b_k\}$  in which, at each time  $t = kT$ , where  $k$  is an integer, one (no) electron is injected if  $b_k = 1$  [ $b_k = 0$ ; see Fig. 1(a)]. This provides a situation intermediate between the periodic and single-electron injections. Also a binary injection is what we have to be prepared to do for flying-qubit operation in electron quantum optics. This is thus a field of investigation that may be worth

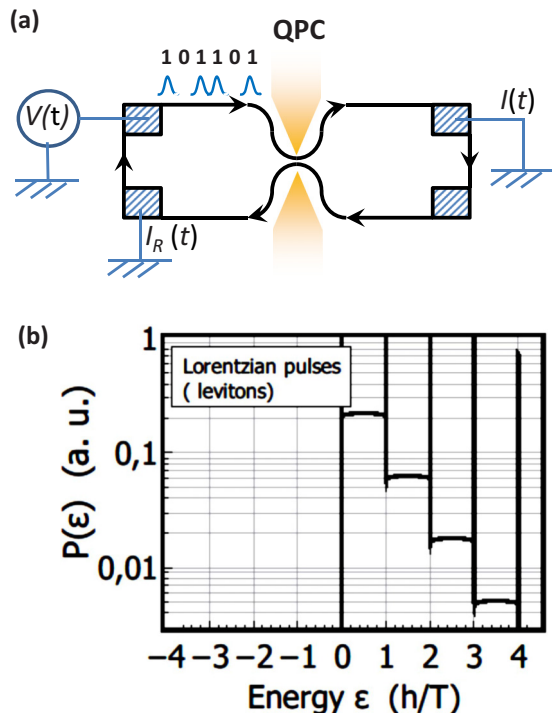


FIG. 1. (a) Chiral ballistic conductor with a quantum point contact in its middle playing the role of a beam splitter of transmission  $D$ . The voltage  $V(t)$  injects levitons through a series of Lorentzian voltage pulses following a pseudorandom binary bit sequence. (b) The probability  $P(\varepsilon)$  to shift by  $\varepsilon$  the energy of electrons experiencing a pseudorandom binary sequence of Lorentzian voltage pulses is computed from the FT of Eq. (18). The single-sideband energy spectrum [ $P(\varepsilon) = 0$  for  $\varepsilon < 0$ ] is characteristic of Lorentzian voltage pulses. It guarantees that only electron like excitations are generated by the pulses, as expected for leviton generation. This generalizes to random emission results found for periodic injection.  $W = 0.1T$  here.

developing. Regarding pure-physics concerns, a direct result of random injection is to spread the energy spectrum and remove the  $h\nu$  singularities. We will show that the electron energy spectrum is made from a continuous part directly related to the statistics of the bit ensemble  $\{b_k\}$  while weaker spectral discontinuities remain which are directly related to the regular bit sequence. Looking at the off-diagonal element of the energy density matrix we will show that these spectral peaks are related to long-range phase coherence. Comparing periodic and random injections provides a tool to better disentangle the physics of injected electrons from the injection physics. In the present work we show that this enables us to better characterize the dynamical orthogonality catastrophe [27] predicted in [13] for noninteger charge injection and to quantify the number of electron-hole pairs created when injecting electrons with non-Lorentzian pulses. Another advantage of nonperiodic injection is found in the case of electronic Hong-Ou-Mandel (HOM) interferometry, which gives the time correlation function of the electron wave function  $|\langle \psi(\tau) | \psi(0) \rangle|^2$ . As we will show below, this allows for better exploration of the tails of the single-electron (leviton) wave function, while periodicity limits this information to a half-period time scale:  $\tau \leq T/2$ .

In a broader perspective, nonperiodic injection belongs to the class of spread-spectrum techniques used in communications, and the problem provides a bridge between quantum physics and telecommunication problems. Indeed, some of the theoretical results derived here are directly imported and adapted from the field of digital communications [28]. Considering the rapid development of periodically or quasiperiodically driven Hamiltonians [29,30], the study of the response of quantum systems to nonperiodic spread-spectrum excitations is only starting [31,32]. It may be viewed as a new field which, except in quantum communication, has not yet been explored and which could shed new (white) light on quantum effects.

## II. BACKGROUND

### A. Floquet scattering approach

Before presenting our approach to deal with this new situation, we recall the main results of the Floquet scattering approach [33] for periodic excitation. The next section will extend the Floquet approach to nonperiodic drive.

We consider a periodic voltage  $V_L(t)$  applied to, say, the left contact of a ballistic conductor while the opposite (right) contact is kept grounded ( $V_R = 0$ ). For simplicity spin is disregarded, and the conductor is made of a single quantum channel [for example, the edge channel of the integer quantum Hall effect as sketched in Fig. 1(a)]. Later, including the spin and generalizing to several electronic modes are straightforward.

According to the scattering approach developed by Moskalets and Büttiker [33], an electron emitted at energy  $E$  below the Fermi energy  $\mu_L$  from the left contact and experiencing the ac excitation has its phase  $\phi(t)$  modulated by the voltage, with

$$\phi(t) = \int_{-\infty}^t eV(t')dt'/h. \quad (1)$$

With the time dependence breaking energy conservation, the emitted electron is scattered into a superposition of quantum states at energies  $E + lh\nu$ , where  $l$  is an integer. The scattering amplitudes connecting initial and final energies are the photoabsorption (emission) amplitudes  $p_l$ , which form the elements of the so-called unitary Floquet scattering matrix, where positive (negative)  $l$  means an electron absorbing (emitting)  $l$  photons. The amplitudes  $p_l$  are given by the Fourier transform of the phase term:

$$p_l = \frac{1}{T} \int_0^T \exp[-i\phi(t)] \exp(i2\pi l\nu t) dt. \quad (2)$$

From unitarity,  $p_l$  obey the following useful identity:  $\sum_l p_{l+k}^* p_l = \delta_{k,0}$ , where the asterisk (\*) denotes the complex conjugate. To calculate transport properties, the standard annihilation fermionic operators  $\hat{a}_L(E)$  which operate on the equilibrium states of the left contact are replaced by new annihilation fermion operators  $\hat{\tilde{a}}_L(E)$ , with  $\hat{\tilde{a}}_L(E) = \sum_l p_l \hat{a}_L(E - lh\nu)$ . This substitution in the transport formula provides a direct expression for the mean photoassisted current  $\tilde{I}$  and mean photoassisted shot noise  $\tilde{S}_I$  related to the dc transport expressions  $I$  and  $S_I$ . Defining  $P_l = |p_l|^2$  as the probability to absorb or emit  $l$  photons and anticipating the case of nonperiodic drive, we define the density of probability per unit

energy as

$$P(\varepsilon) = \sum_l P_l \delta(\varepsilon - lh\nu). \quad (3)$$

We can rewrite the known expression for the average current, the average current noise [34,35], and the electron energy distribution under ac excitation as follows:

$$\tilde{I}(V_{\text{dc}}) = \int_{-\infty}^{+\infty} P(\varepsilon) I(V_{\text{dc}} + \varepsilon/e) d\varepsilon, \quad (4)$$

$$\tilde{S}_I(V_{\text{dc}}) = \int_{-\infty}^{+\infty} P(\varepsilon) S_I(V_{\text{dc}} + \varepsilon/e) d\varepsilon, \quad (5)$$

$$\tilde{f}(\varepsilon) = \int_{-\infty}^{+\infty} P(\varepsilon') f(\varepsilon - \varepsilon' - eV_{\text{dc}}) d\varepsilon', \quad (6)$$

where  $f(\varepsilon)$  is the equilibrium Fermi distribution with energies referred to the right contact Fermi energy and we have added an extra dc voltage  $V_{\text{dc}}$  to the ac voltage  $V(t)$  for generality. A typical application is a single-channel conductor with a QPC in its middle transmitting electrons with transmission probability  $D$ . For energy-independent transmission, giving linear  $I-V$  characteristics, and for  $V(t)$  having zero mean value, remarkably,  $\tilde{I}(V_{\text{dc}}) = I(V_{\text{dc}})$ , where  $I(V_{\text{dc}}) = D(e^2/h)V_{\text{dc}}$  is, according to the Landauer formula, the dc current that we would measure when only a dc bias  $V_{\text{dc}}$  was applied to the left contact. Indeed, from unitarity  $\sum_l P_l = 1$ , while  $\sum_l l P_l = 0$ . By contrast, the shot noise shows a nonlinear (rectificationlike) variation with current (or voltage). Indeed, the zero-temperature shot noise is  $S_I = 2e \frac{e^2}{h} |V_{\text{dc}}| D(1-D)$  [36–38], where the  $D(1-D)$  factor encodes the partitioning of an electron between transmitted and reflected states with binomial statistics. From Eq. (5), the singular  $P(\varepsilon)$  for periodic drive gives a replica of the zero-bias singularity in the photoassisted shot noise  $\tilde{S}_I$  each time  $V_{\text{dc}} = lh\nu$  [34,35,39–41]. The singularities result from stepwise variations of the energy distribution  $\tilde{f}(\varepsilon)$  of the periodically driven Fermi sea given by

$$\tilde{f}(\varepsilon) = \sum_l P_l f(\varepsilon - lh\nu - eV_{\text{dc}}), \quad (7)$$

where  $f(\varepsilon) = 1/[1 + \exp(\beta(\varepsilon - \mu))]$  is the Fermi Dirac distribution of electrons at electronic temperature  $k_B T_e = 1/\beta$  with the right contact Fermi energy  $\mu$  taken as the energy reference. Terms with positive (negative)  $l$  describe electronlike (holelike) excitations.

As shown in [13,14,16] and detailed in [24], a particular situation arises when the voltage  $V(t)$  is a sum of periodic Lorentzian pulses,

$$V(t) = \frac{h}{\pi e T} \sum_{k=-\infty}^{+\infty} \frac{1}{1 + (t - kT)^2/W^2}, \quad (8)$$

where each introduces a single electron in the conductor. Here  $P_l$  remarkably vanish for  $l < 0$ , and  $\tilde{f}(\varepsilon)$  describes a pure electron excitation population with no holes. This defines a *minimal excitation state* [16] made of a periodic train of *levitons* [11].

When partitioning the leviton train, the shot noise, which is proportional to the total number of excitations [24], is minimal due to the absence of holes. In general, arbitrarily shaped (non-Lorentzian) voltage pulses give nonzero  $P_l$  for negative  $l$  and thus generate a mixture of electron and hole excitations.

This is, for example, the case for sine-wave voltage pulses  $V(t) = (h\nu/e)[1 - \cos(2\pi\nu t)]$  injecting single electrons. The qualitative difference between Lorentzian voltage pulses and other pulse shapes is that the modulated phase gives a single-sideband (SSB) energy spectrum [only positive (negative) energies for electronlike (holelike) levitons]. All other kinds of modulation give a double-sideband spectrum. Having a SSB spectrum property with positive (negative) energy requires that  $\exp[i\phi(t)]$  has no poles in the upper (lower) half of the complex plane. This is the case for the periodic injection of levitons, where

$$\exp[i\phi(t)] = \frac{\sin[\pi(t + iW)/T]}{\sin[\pi(t - iW)/T]} \quad (9)$$

shows periodically spaced poles in the upper complex plane.

### B. Nonperiodic Floquet scattering

We now address nonperiodic excitations leading to the spread-spectrum property. As the term ‘‘Floquet’’ is associated with purely periodic phenomena, ‘‘nonperiodic Floquet scattering’’ may appear to be an oxymoron. However, the Floquet concept has already been extended beyond periodicity. Recently, there has been considerable activity regarding topological phase transitions where, using incommensurate frequencies, the biharmonic driving of the Hamiltonian leads to new topological Floquet lattices and energy bands [29,30]. In fact, for quantum systems the Floquet approach is essentially a way to describe scattering in energy. This is why, for quantum conductors, the Moskalets-Büttiker Floquet scattering approach [33] integrates so well within the Landauer-Büttiker scattering transport approach.

For nonperiodic driving, the photoabsorption probabilities become a continuous function of the energy. In this spread-spectrum situation, the definition of the photoabsorption or emission probability amplitudes becomes

$$p(\varepsilon) = \int_{-\infty}^{+\infty} dt \exp[-i\phi(t)] \exp(i\varepsilon t/\hbar). \quad (10)$$

This describes the amplitude needed to find an electron initially emitted by the reservoir at energy  $E$  scattered with the energy  $E + \varepsilon$ . From this one can calculate the statistical average of  $|p(\varepsilon)|^2$ , giving the probability  $P(\varepsilon)$  from which current, shot noise, and energy distribution can be calculated using expressions similar to Eqs. (4)–(6). A similar use of these expressions for fully random excitations that is appropriate for interacting systems can be found in [31].

## III. BINARY INJECTION OF LEVITONS

### A. Energy scattering probability

The pseudorandom injection leads to a continuous spectrum characterized by an energy scattering probability  $P(E)$  that we derive in this section and which is the analog of the photoabsorption/emission probability considered above for the periodic voltage drive.

As a realistic practical example, we consider the injection of single-charge levitons following a pseudorandom sequence of binary bits  $b_k = 0, 1$ . The voltage drive applied on the left

contact is thus

$$V(t) = \frac{\hbar}{\pi e T} \sum_{k=-\infty}^{+\infty} \frac{b_k}{1 + (t - kT)^2/W^2}. \quad (11)$$

The mean value of the drive voltage is  $\langle b_k \rangle eh/T$ , where  $\langle b_k \rangle$  is the ensemble average of the bit value, typically 0.5 for equal-bit pseudorandom probability. The phase term  $\exp[i\phi(t)]$  corresponding to the pseudorandom binary levitonic drive is given by

$$\exp[i\phi(t)] = \prod_{k=1}^N \left( \frac{t - kT + iW}{t - kT - iW} \right)^{b_k}. \quad (12)$$

The problem of calculating  $P(\varepsilon)$  is similar to the calculation of the power spectrum density in digital communication for binary phase pulse modulation (see [28,42]). In this analogy, the electronic quantum phase corresponds to the modulated phase, the voltage pulses correspond to frequency pulses, the energy corresponds to frequency, and  $P(\varepsilon)$  corresponds to electromagnetic power. To obtain  $P(\varepsilon)$ , one needs the two-time autocorrelation function:

$$\langle C(t, t') \rangle = \langle \exp[-i\phi(t)] \exp[i\phi(t')] \rangle, \quad (13)$$

where  $\langle \cdot \rangle$  means ensemble averaging over statistically independent bit patterns. One can show that  $\langle C(t, t') \rangle$  is cyclostationary; that is,  $\langle C(\bar{t} + \tau/2, \bar{t} - \tau/2) \rangle$  is invariant when  $\bar{t} \rightarrow \bar{t} + T$ , where  $\bar{t} = (t + t')/2$  is the mean time and  $\tau = t - t'$  is the time difference. After averaging over  $\bar{t}$  we get the time-average correlation function  $\langle \overline{C(\tau)} \rangle$ , whose Fourier transform (FT) gives

$$P(\varepsilon) = (h/T) \int_{-\infty}^{+\infty} \langle \overline{C(\tau)} \rangle e^{i\varepsilon\tau/\hbar} d\tau. \quad (14)$$

We now derive the expressions from which these physical quantities can be calculated. We will set  $T = 1$  and  $\tau$  and  $\bar{t}$  in period units and  $w = W/T$ , and we consider the ensemble  $\{b_k\}$  as uncorrelated Bernoulli random variables with probabilities  $P[b_k = 1] = p$  and  $P[b_k = 0] = 1 - p$ .

The two-time autocorrelation function is

$$C\left(\bar{t} - \frac{\tau}{2}, \bar{t} + \frac{\tau}{2}\right) = \prod_{k=-\infty}^{\infty} \left( \frac{t_k - \frac{\tau}{2} - iw}{t_k - \frac{\tau}{2} + iw} \frac{t_k + \frac{\tau}{2} + iw}{t_k + \frac{\tau}{2} - iw} \right)^{b_k}, \quad (15)$$

where  $t_k = \bar{t} - k$ . After averaging over statistically equivalent bit sequences, we get

$$\begin{aligned} & \langle C(\bar{t} + \tau/2, \bar{t} - \tau/2) \rangle \\ &= \prod_k \left( 1 - p + p \frac{t_k^2 - (iw + \frac{\tau}{2})^2}{t_k^2 - (iw - \frac{\tau}{2})^2} \right) \\ &= \frac{\sin[\pi(\bar{t} - \theta_p(\tau))] \sin[\pi(\bar{t} + \theta_p(\tau))]}{\sin[\pi(\bar{t} - iw + \frac{\tau}{2})] \sin[\pi(\bar{t} + iw - \frac{\tau}{2})]}, \quad (16) \end{aligned}$$

where  $\theta_p(\tau) = \sqrt{\frac{\tau^2}{4} - w^2 - (1 - 2p)iw\tau}$ . Note that Eq. (16) interpolates between no modulation ( $p = 0$ , all  $\{b_k = 0\}$ , and  $C$  is constant) and the periodic case ( $p = 1$ ). Remarkably, Lorentzian pulses (levitons) give rise to analytical expressions

of the correlation functions. The two-time correlation function can be written as

$$\langle C(\bar{t} + \tau/2, \bar{t} - \tau/2) \rangle = \frac{\cos[2\pi\theta_p(\tau)] - \cos(2\pi\bar{t})}{\cos 2\pi(\tau/2 - iw) - \cos(2\pi\bar{t})}. \quad (17)$$

As expected, it shows a cyclostationary property. Its time average is

$$\langle \overline{C(\tau)} \rangle = 1 + \frac{\cos[2\pi\theta_p(\tau)] - \cos[\pi(\tau - 2iw)]}{\sin[\pi(\tau - 2iw)]}. \quad (18)$$

The first part of the numerator of Eq. (18), with  $\theta_p(\tau)$  in the cosine argument is responsible for a continuous spectrum, as expected for random excitation, and depends, via the parameter  $p$ , on the statistics of the bit injection. The second part represents harmonic contributions giving lines in the energy spectrum, reflecting the regularity of injection. Finally, the imaginary part in the argument of the sine term in the denominator indicates that  $C(\tau)$  has only poles in the top half of the complex plane and no poles in the lower part and ensures that  $P(\varepsilon)$ , its FT, vanishes for negative energies, as expected for levitons. Figure 1(b) shows the variations of  $P(\varepsilon)$  for  $w = W/T = 0.1$  and  $p = 1/2$ , corresponding to equal-bit probability. The energy spectrum is continuous with spectral lines at energies of multiple  $h/T$  and extends only to positive energies.

For comparison we consider similar pseudorandom binary injection of single electrons but with square-wave voltage pulses, with  $V(t) = \sum_k b_k V_0(t - kT)$ , where  $V_0(t) = (2h/eT)$  if  $t \in [0, T/2]$  and  $V_0 = 0$  for  $t \in [T/2, T]$ . Expressing  $\varepsilon$  in reduced units of  $h/T$ , we found  $P(\varepsilon)$  given by

$$\begin{aligned} P(\varepsilon) &= \frac{1}{4} \left[ \left( \frac{\sin(\pi\varepsilon/2)}{(\pi\varepsilon/2)(2-\varepsilon)} \right)^2 + \frac{9}{4}\delta(\varepsilon) + \frac{1}{4}\delta(2-\varepsilon) \right. \\ &\quad \left. + \sum_{p=-\infty}^{+\infty} \frac{4}{\pi^2} \frac{1}{(2p^2-1)^2} \delta(2p+1-\varepsilon) \right]. \quad (19) \end{aligned}$$

As for the levitons, the first term gives a continuous energy spectrum followed by a series of lines at multiples of the characteristic energy  $h/T$ . One can show (see [28]) that the first term is  $\propto \langle b_k^2 \rangle - \langle b_k \rangle^2$ , which is  $1/4$  here, and results from the fluctuating part of the injection making the spectrum continuous, while the next terms, the spectral line,  $\propto \langle b_k \rangle^2$ , result from the regular part of the injection. Figure 2(a) shows the continuous part of  $P(\varepsilon)$  calculated from Eq. (19) and the results of the numerical simulations.

The Dirac peaks in the energy scattering probability  $P(E)$  are not the sole result of regular injection but are intimately related to the integer charge. From the field of digital communication, where the bit information is coded by phase modulation, it is known that similar peaks in the emission power of digital phase modulation also appear when the so-called modulation index  $h$  is an integer, i.e., when the phase increment  $\Delta\phi = h2\pi$  associated with an elementary frequency pulse is a multiple of  $2\pi$  (see [28], Chap. 3). A  $2\pi$  phase increment is exactly what is imprinted on the electronic phases when integer charges are injected. Indeed, using  $I(t) = \frac{e^2}{h} V(t)$ , one finds  $\Delta\phi/2\pi = \int_0^T dt eV(t)/h = \int_0^T I(t)dt = q$ . To suppress the peaks which carry useless energy, telecommunication engineers prefer to

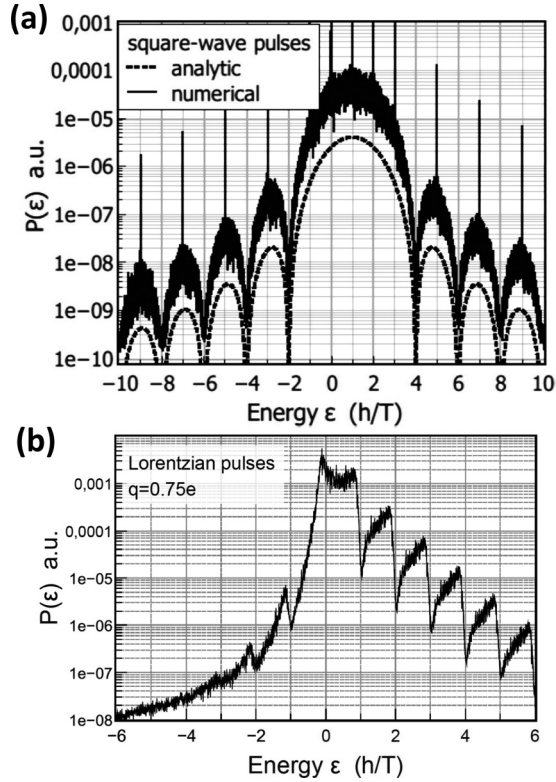


FIG. 2. (a)  $P(\varepsilon)$  for single electrons injected with pseudorandom binary square-wave voltage pulses of length  $T/2$ . The dashed curve is the continuous part of the analytic expression (19). The upper noisy curve is from numerical simulations, where eight spectra made of 1024 uncorrelated bit patterns are averaged. For clarity a vertical shift between curves has been made by applying a different arbitrary scale factor to the curves. The double-sideband energy spectrum shows that square-wave pulses, unlike levitonic pulses, generate holelike excitations, as already observed for periodic injection. (b)  $P(\varepsilon)$  for binary random Lorentzian voltage pulses injecting a noninteger charge. The absence of sharp peaks observed for integer charge is characteristic of fractional charge pulses. Although the pulses are Lorentzian, noninteger pulse are not minimal excitation states as the energy spectrum is a double sideband signaling holelike excitations.

use a noninteger modulation index. In electron language, suppression of peaks will occur for noninteger charge injection as the electronic wave modulation index is  $h = q/e$ . This is shown in Fig. 2(b) for random binary Lorentzian voltage pulses carrying charge  $q = 0.75e$ . We see here an example where nonperiodic injection leads to physical manifestations not observable in the case of simple periodic injection.

### B. Quantum coherence of pseudorandom injection

From a superficial inspection one might conclude that the random injection, like thermal injection, will lead to incoherent charge states. Here we show that this is not the case. As observed in the case of periodic injection, the density matrix in the energy representation presents significant off-diagonal components, a signature of coherence of the injected leviton train. While for the thermal emission of electrons by a contact there is no phase relation between two injected electrons, by contrast, the regular pseudorandom injection of an integer

charge is shown to preserve phase coherence between electrons.

Let's first consider the case of pure periodic injection. We start from the first-order electron coherence  $g_1(t', t) = \langle \psi^\dagger(t')\psi(t) \rangle$  [25,43,44], where the brackets here indicate the quantum statistical average and the Fermionic electron operator  $\psi$  describing the injected electrons is  $\psi(t) = \int_{-\infty}^{+\infty} d\varepsilon \hat{a}_L(E) e^{-i\varepsilon t}$ . We consider a linearized dispersion relation;  $t$  is shorthand notation for  $t - x/v_{\text{Fermi}}$ , and  $\hat{a}_L(E)$ , defined above, describes the annihilation operator of electrons that experienced the voltage pulse. Using the energy representation  $\psi(\varepsilon_0) = \int_{-\infty}^{+\infty} dt \psi(t) e^{i\varepsilon_0 t}$ , we focus on the elements  $\rho(\varepsilon', \varepsilon)$  of the electron density matrix in the energy representation:

$$\rho(\varepsilon', \varepsilon) = \langle \psi^\dagger(\varepsilon')\psi(\varepsilon) \rangle - \langle \psi^\dagger(\varepsilon')\psi(\varepsilon) \rangle_{\text{FS}}. \quad (20)$$

$\rho$  is directly related to the first-order coherence via  $g_1(t', t) = \int_{-\infty}^{+\infty} d\varepsilon' d\varepsilon e^{i(\varepsilon' t' - \varepsilon t)} \rho(\varepsilon', \varepsilon)$ . The second term on the right-hand side represents the subtraction of the Fermi sea (FS) contribution. Using the expression of  $\hat{a}_L(E)$  for periodic injection, one finds

$$\rho(\varepsilon', \varepsilon) = [\tilde{f}(\varepsilon) - f(\varepsilon)]\delta(\varepsilon - \varepsilon') + \sum_{k \neq 0} \tilde{f}_k(\varepsilon) \delta(\varepsilon' - \varepsilon - kh\nu). \quad (21)$$

The first term on the right-hand side is the diagonal term representing the energy distribution as in Eq. (6), but with the FS subtracted. The last term with  $\tilde{f}_k(\varepsilon) = \sum_l p_{l-k}^* p_l f(\varepsilon - lh\nu)$  describes the nondiagonal terms. They characterize the coherence of the injection. They were recently measured in order to perform the quantum state tomography of periodic leviton trains in Ref. [12]. The nondiagonal terms are responsible for long-range correlation between times  $t'$  and  $t$  in  $g_1(t', t)$ .

The fact that, for periodic drive, there are nonzero diagonal terms  $\tilde{f}_k$  linking energies separated by  $kh\nu$  was found in deriving Eq. (21) originating from the cyclostationary two-time correlation function  $C(t', t) = \exp[-i\phi(t)] \exp[i\phi(t')]$ , with mean time  $\bar{t} = (t + t')/2$  and relative time  $\tau = t - t'$ :

$$C(t', t) = \sum_k C_k(\tau) e^{-ik2\pi v \bar{t}}, \quad (22)$$

where  $C_k(\tau) = e^{ik\pi v \tau} \sum_l p_{l-k}^* p_l e^{il2\pi v \tau}$ .

Similarly, for pseudorandom leviton injection we have found that the two-time correlation function  $C(t', t)$  is cyclostationary after averaging over an ensemble of random-bit realizations. From this observation, we can define the following relative time correlation functions  $\langle C_k(\tau) \rangle$ :

$$\langle C(t', t) \rangle = \sum_k \langle C_k(\tau) \rangle e^{-ik2\pi v \bar{t}}, \quad (23)$$

where we found that  $\langle C_k(\tau) \rangle = e^{ik2\pi \tau} e^{-k2\pi w} \langle C_0(\tau) \rangle$  and  $\langle C_0(\tau) \rangle$  was given in Eq.(18). We show here that despite the injection randomness the cyclostationary property leads to finite off-diagonal density-matrix elements for energy separated by the quantity  $kh\nu$ .

The continuous version of Eq. (21) is given by

$$\rho(\varepsilon', \varepsilon) = \int_{-\infty}^{\infty} dE \tilde{f}_E(\varepsilon) \delta(\varepsilon' - \varepsilon - E), \quad (24)$$

where the nondiagonal energy density term is

$$\tilde{f}_E(\varepsilon) = \int_{-\infty}^{+\infty} dE' p^*(E' - E) p(E') f(\varepsilon - E') \quad (25)$$

and  $p(E') = \frac{1}{2\pi} \int_{-\infty}^{+\infty} dt e^{-i\phi(t)} e^{iE't}$ . Averaging Eq. (25) over bit ensembles and using (23), we find that

$$\tilde{f}_E(\varepsilon) = \frac{\delta(E - kh\nu)}{2\pi} \int_{-\infty}^{+\infty} dE' \int_{-\infty}^{+\infty} d\tau \langle C_k(\tau) \rangle f(\varepsilon - E'). \quad (26)$$

Thus, nondiagonal elements connect energies separated by the amount  $h\nu$  as in the periodic drive case.

Having shown the coherent character of a train of randomly injected levitons, we would like to discuss its meaning. Off-diagonal coherence is related to the cyclostationarity of the two-time correlation functions of the phase variation imprinted on the electronic wave function. It is related to the regular periodic bit injection. If the time  $T$  between two injections were random, the cyclostationary character of the injection statistics would be lost. The regular injection ensures that two levitons injected at distant times keep a well-defined temporal phase and hence preserves the coherence property. In general, it does not seem possible to mimic a thermal electron source by an appropriate modulation of the voltage  $V(t)$  applied on a contact. An attempt to find a voltage pulse shape creating an electron-hole diagonal energy distribution similar to a Fermi distribution can be found in [45]. However, off-diagonal terms show that this distribution is not like that of a thermal distribution, as signaled by the vanishing noise for perfect channel transmission, in contrast to the finite thermal noise.

Finally, the notation  $P(E)$ , which describes scattering in energy, may be confused with the  $P(E)$  notation used to describe dynamical Coulomb blockade (DCB). In the latter case  $P(E)$  describes the energy scattering due to the back-action of electron shot noise, which, under finite impedance, the external circuit transforms into random incoherent voltage fluctuations. Because of the fully random voltage fluctuations no off-diagonal density-matrix elements should be expected, and the phenomenon is purely incoherent. We consider here the only useful experimental situation where the external circuit impedance, typically  $50 \Omega$ , is negligible, and this DCB interaction regime is disregarded.

#### IV. QUANTIFYING ELECTRON-HOLE EXCITATIONS

##### A. Levitons versus nonminimal integer charge pulses

It is interesting to quantify the number of excitations per pulse generated by the random pulses and compare the result with the periodic case. The number of electrons (holes)  $N_e$  ( $N_h$ ) created per pulse is given by  $N_e = \int_0^{\infty} \varepsilon P(\varepsilon) d\varepsilon$  [ $N_h = \int_{-\infty}^0 (-\varepsilon) P(\varepsilon) d\varepsilon$ ] while the average charge per pulse is  $\langle q \rangle = e(N_e - N_h)$ . With these definitions, the number of extra excitations accompanying the injected charge is  $\Delta N_{\text{exc}} = N_e + N_h - \langle q \rangle$  per pulse. In terms of  $P(\varepsilon)$ ,

$$\langle q \rangle = \int_{-\infty}^{+\infty} P(\varepsilon) \varepsilon d\varepsilon, \quad (27)$$

$$N_e + N_h = \int_{-\infty}^{+\infty} P(\varepsilon) |\varepsilon| d\varepsilon, \quad (28)$$

TABLE I.  $\Delta N_{\text{exc}}/\langle q \rangle$ , the number of electron-hole pairs per mean injected charge  $\langle q \rangle$ . Equal-bit probability is assumed here.

Injection	$\langle q \rangle$	Lorentzian	Sine pulse	Square pulse
Periodic	1	0	0.028	0.1082
Pseudorandom	0.5	0	0.0548	0.1289

$N_e + N_h$  can be measured using shot noise measurements [see Eq. (5)]. This was experimentally demonstrated in [11]. Indeed, if the charges injected by the pulses in a ballistic conductor are sent to a beam splitter with transmission  $D$ , their partitioning gives the zero-temperature noise  $S_I = 2[e^2(e/T)]D(1-D)(N_e + N_h)$  [24]. We now compare various single-charge voltage pulses. In the following equal-bit probability is assumed for all pulse shapes. The computation of (27) from  $P(\varepsilon)$  gives the same average charge  $\langle q \rangle = e/2$  per injection period, trivially resulting from equal-bit probability. The Lorentzian pulses give no extra excitation  $\Delta N_{\text{exc}} = 0$ , as expected, while the square-wave pulses give  $\Delta N_{\text{exc}}/\langle q \rangle = 0.1289$ . This should be compared with the periodic square-wave case in [11,24], which found  $\Delta N_{\text{exc}}/\langle q \rangle = 0.1082$ . We have also numerically computed the case of the sine-wave voltage pulse injection where, during a period  $T$ ,  $V(t) = \sum_k b_k (h/eT) [1 - \cos 2\pi(t - kT)/T]$ . One finds  $\Delta N_{\text{exc}}/\langle q \rangle = 0.05476$  (and  $\langle q \rangle = e/2$ ), while for the periodic case one has  $\Delta N_{\text{exc}}/\langle q \rangle = 0.028$  (and  $\langle q \rangle = 1$ ). This confirms that sine-wave pulses produce fewer extra excitations than square-wave pulses, but in both cases the pseudorandom binary injection generates more excitations per charge injected than the periodic injection. From this study *we learn that the number of extra excitations not only is a property of a given (single) pulse shape* but also depends on the way the pulses are injected. The values of the number of extra electron-hole pair excitations per pulse  $\Delta N_{\text{exc}}/\langle q \rangle$  are summarized in Table I.

##### B. Fractional charge pulses

The discrepancy between periodic and binary injection becomes more pronounced if we consider noninteger pulses. Indeed, the injection of pulses carrying noninteger charge can never give rise to a minimal excitation state, even in the case of Lorentzian voltage pulses. For nonminimal excitation pulses, like sine- or square-wave pulses, this also manifests as a cusp in the electron-hole number per pulse versus pulse charge when the charge crosses an integer value (see Fig. 6 in [24]). This strong result is related to the so-called dynamical orthogonality catastrophe (DOC) discussed in [13]. The orthogonality catastrophe, first introduced by Anderson for static impurities [27], means that the electronic wave phase shift resulting from the presence of the impurity makes the Fermi sea with impurity orthogonal to the Fermi sea without impurity. The dynamical orthogonality catastrophe [13] is similar but for a dynamical phase shift. This occurs when the phase shift generated by a voltage pulse is not a multiple of  $2\pi$  (i.e., for a noninteger modulation index  $h$  or for a pulse carrying a noninteger charge  $q$ ). This tells us that injecting a noninteger charge in a noninteracting Fermi system can be done only at the expense of a large superposition of electron and hole excitations.

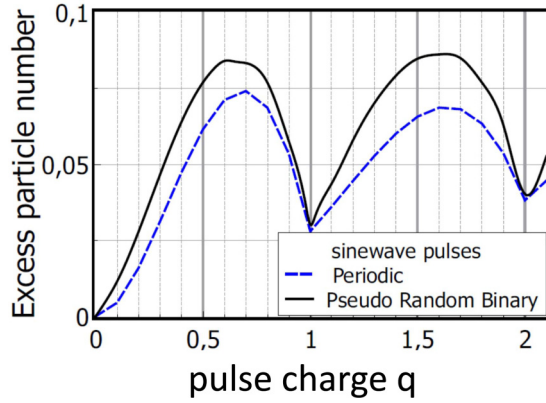


FIG. 3. Comparison of the excess number of excitations  $\Delta N_{\text{exc}}$  produced per period for sine-wave pulses carrying charge  $q$  for periodic and binary pulse injections.  $\Delta N_{\text{exc}}$  shows local minima for integer charges, while for noninteger charge it grows as a result of the dynamical orthogonality catastrophe (DOC). Random binary injection giving more excitations than periodic injection is consistent with the DOC scenario as, on average, separation between pulses is larger.

In particular, the number of excited particle-hole pairs detected over a large time interval  $t$  diverges as  $\ln(t/W)$  [13,46,47], where  $W$  is the time for switching the perturbation and is typically the width of Lorentzian pulses here. In general, more space between pulses gives more freedom to the excited Fermi sea to create extra excitations. Thus, for binary injection, with the average waiting time between injected wave packets being larger than in the periodic case, one expects to observe more particle-hole excitation per pulse.

Results are given here for sine-wave pulses in Fig. 3, which displays the evolution of  $\Delta N_{\text{exc}}$  versus the charge  $q$  per pulse for periodic and nonperiodic binary injection using  $eV(t) = \sum_k b_k(qh/T)[1 - \cos(2\pi(t - kT)/T)]$ . For noninteger charge value, the number of electron-hole excitations clearly rises, signaling the dynamical orthogonality catastrophe. For perspective, a similar study could shed light on the curious properties of fractional charge pulses [26,48] and on the recently considered half levitons [49], which are singular zero-energy fractional excitations minimizing noise in superconducting normal junctions [50].

## V. HONG-OU-MANDEL INTERFERENCE WITH PSEUDORANDOM BINARY PULSES

Finally, we address electronic HOM correlations where identical binary sequences of Lorentzian pulses are applied

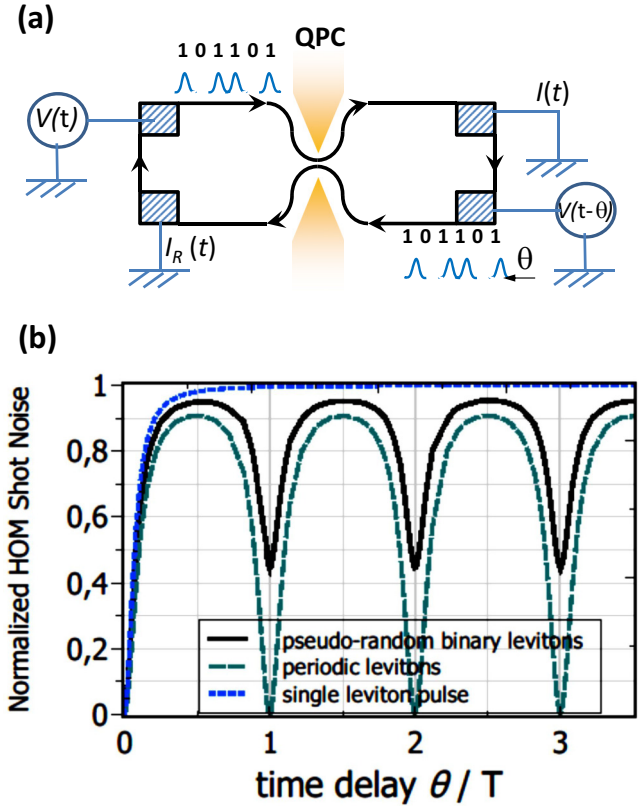


FIG. 4. (a) Schematic of Hong-Ou-Mandel shot noise for levitons colliding in a beam splitter with time delay  $\theta$ . (b) The binary (solid line), periodic (dashed line), and single-pulse (dotted line) injections are compared for  $W = 0.35T$ . Although periodic injection limits the information in the range  $[0, T/2]$ , information for a larger time scale is given by the binary injection, whose variation at small  $\theta$  is closer to that of a single pulse. Periodic HOM dips appearing for  $\theta$  multiples of  $T$  result from the occurrence of bits (0,0) and (1,1), each with a 25% probability of giving an  $\sim 50\%$  HOM dip.

on opposite contacts of a QPC forming a beam splitter with transmission  $D$  [see Fig. 4(a)]. We introduce a time delay  $\theta$  between the two voltages  $V_L(t) = V^{\text{bin}}(t - \theta/2)$  and  $V_R(t) = V^{\text{bin}}(t + \theta/2)$ . The measure of the HOM interference is given by the noise  $S_I^{\text{HOM}}(\theta) \propto [1 - |\langle \psi(\theta) | \psi(0) \rangle|^2]$  observed in the current fluctuation of the output leads resulting from two-electron partitioning, as shown for periodic electron injection in [11,21]. The time correlation function  $\langle \overline{C}(\tau, \theta) \rangle$  enabling calculation of  $P(\varepsilon)$ , as done in Eq. (14), is

$$\langle \overline{C}(\tau, \theta) \rangle = 1 + I(\tau, \theta) + I(\tau, -\theta)^*, \quad (29)$$

$$I(\tau, \theta) = \frac{i}{2} [\cos 2\pi(\tau + \theta/2 - iw) - \cos 2\pi\tau] \times \frac{[\cos 2\pi(\tau + \theta/2 + iw) - \cos 2\pi\tau]}{\sin 2\pi(\tau - \theta/2 + iw) \sin 2\pi\tau \sin 2\pi(\theta/2 - iw)}, \quad (30)$$

where

$$t^\pm = \{\tau^2 + (\theta/2)^2 - w^2 \pm \sqrt{4\tau^2[(\theta/2)^2 - w] - (w\theta/2)^2}\}^{1/2}. \quad (31)$$

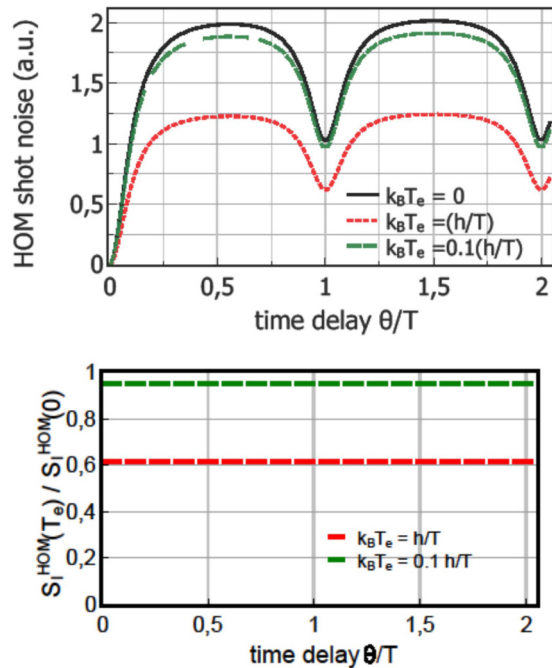


FIG. 5. Top: Hong-Ou-Mandel shot noise for levitons colliding in a beam splitter with time delay  $\theta$  and  $W = 0.05T$  for different electronic temperatures  $T_e$ . Bottom: The ratio between curves shows that they are homothetic: remarkably, the shape of the HOM noise curve versus time delay is not affected by temperature, except an overall reduction factor, as already observed for periodic injection.

The HOM noise is shown in Fig. 4. For  $\theta = 0$  electrons emitted by identical sequences are indistinguishable at all times. The Fermi statistics leads to perfect antibunching, and 100% noise suppression is found. We see a replica of the noise suppression, only 50% deep, for  $\theta = kT$ , which corresponds to (0,0) and (1,1) bit events each occurring with 25% probability. These dips could be reduced by one half using binary Barker codes [51] characterized by a sharply peaked correlation function  $\langle b_k b_{k+p} \rangle$  at  $p = 0$ . The HOM noise of periodic levitons is shown for comparison, along with the single-pulse HOM noise. The pseudorandom binary injection is in between and provides information on the leviton not limited to  $\theta \leq T/2$ . To complete this study we generalize to random injection the remarkable result, found for periodic injection in [24] and observed in [52], that the HOM leviton noise shape versus  $\theta$  is not affected by temperature, a property not shared by sine- or square-wave charge pulses. This is a robust property which has also been theoretically observed in [53] in the interacting regime of the fractional quantum Hall effect where chiral edge channels form Luttinger liquids. This confirms the prediction of [54] that finite temperature, unlike decoherence, does not affect leviton HOM correlations. This is shown in Fig. 5, which demonstrates the homothetic property of HOM noise curves for different temperatures. Finally, it will be interesting

to consider the HOM noise resulting from interference of pseudorandom multiple-charge levitons, that is,  $b_k = 0, 1, 2, 3$ . While we expect zero HOM noise at zero delay, the HOM dip replica should be different from the case of a single charge considered here. In the periodic case, the HOM noise of doubly charged levitons interfering in a quantum point contact was theoretically derived and experimentally observed in [55]. It would be interesting to look at the effect of pseudorandom injection for multiple-charge leviton HOM interference in the fractional quantum Hall regime in view of the recent theoretical observation of crystallized leviton wave packets in this interacting regime [56].

## VI. CONCLUSION

We have generalized the Floquet scattering approach to the nonperiodic driving regime of a quantum conductor. We have given the analytic form of the time correlation function for the binary pseudorandom injection of levitons and for other charge pulses carrying integer charge. We have found the counterintuitive result that a random, but regular, injection does not spoil the coherence of wave packets as signaled by finite off-diagonal elements of the energy density matrix. For noninteger charge pulses we found that the number of neutral electron-hole excitations accompanying the pulses increases compared with the periodic injection as a result of the dynamical orthogonality catastrophe. Considering the Hong-Ou-Mandel interference of pseudorandom integer levitons, we found additional HOM dips resulting from the statistical antibunching of electrons, and we have confirmed the striking robust temperature-independent HOM shape versus time delay.

Considering random injection provides a new tool leading to tractable theoretical results to get new information not accessible in periodic injection. Further studies may include varying the bit injection probability to provide a systematic study of the DOC or using the binary injection to simulate flying-qubit operation. We think this work may also be of interest for the growing community studying Floquet driven Hamiltonians and may give them new perspectives. We hope that this work will inspire new studies exploiting spread-spectrum approaches to get new information on electronic and nonelectronic quantum systems.

## ACKNOWLEDGMENTS

The ANR FullyQuantum Grant No. 16-CE30-0015 and ERC C-Levionics Proof-of-Concept Grant No. 680875 and useful discussions with J. Palicot, Y. Louet, C. Moy, H. Fares, and C. Bader, with I. Safi and D. Ferraro, and with the CEA Saclay Nanoelectronics team are acknowledged.

[1] Y. Ji, Y. Chung, D. Sprinzak, M. Heiblum, D. Mahalu, and H. Shtrikman, An electronic Mach-Zehnder interferometer, *Nature (London)* **422**, 415 (2003).

[2] P. Roulleau, F. Portier, P. Roche, A. Cavanna, G. Faini, U. Gennser, and D. Mailly, Direct Measurement of the Coherence Length of Edge States in the Integer



- Quantum Hall Regime, *Phys. Rev. Lett.* **100**, 126802 (2008).
- [3] A. Bertoni, P. Bordone, R. Brunetti, C. Jacoboni, and S. Reggiani, Quantum Logic Gates Based on Coherent Electron Transport in Quantum Wires, *Phys. Rev. Lett.* **84**, 5912 (2000).
- [4] R. Ionicioiu, G. Amaratunga, and F. Udrea, Quantum computation with ballistic electrons, *Int. J. Mod. Phys.* **15**, 125 (2001).
- [5] S. Hermelin, S. Takada, M. Yamamoto, S. Tarucha, A. D. Wieck, L. Saminadayar, C. Bäuerle, and T. Meunier, Electrons surfing on a sound wave as a platform for quantum optics with flying electrons, *Nature (London)* **477**, 435 (2011).
- [6] R. McNeil, M. Kataoka, C. Ford, C. Barnes, D. Anderson, G. Jones, I. Farrer, and D. Ritchie, On-demand single-electron transfer between distant quantum dots, *Nature (London)* **477**, 439 (2011).
- [7] J. D. Fletcher, P. See, H. Howe, M. Pepper, S. P. Giblin, J. P. Griffiths, G. A. C. Jones, I. Farrer, D. A. Ritchie, T. J. B. M. Janssen, and M. Kataoka, Clock-Controlled Emission of Single-Electron Wave Packets in a Solid-State Circuit, *Phys. Rev. Lett.* **111**, 216807 (2013).
- [8] S. Ryu, M. Kataoka, and H.-S. Sim, Ultrafast Emission and Detection of a Single-Electron Gaussian Wave Packet: A Theoretical Study, *Phys. Rev. Lett.* **117**, 146802 (2016).
- [9] N. Ubbelohde, F. Hohls, V. Kashcheyevs, T. Wagner, L. Fricke, B. Kästner, K. Pierz, H. W. Schumacher, and R. J. Haug, Partitioning of on-demand electron pairs, *Nat. Nanotechnol.* **10**, 46 (2015).
- [10] G. Fève, A. Mahe, J.-M. Berroir, T. Kontos, B. Plaçais, D. C. Glatli, A. Cavanna, B. Etienne, and Y. Jin, An on-demand coherent single-electron source, *Science* **316**, 1169 (2007).
- [11] J. Dubois, T. Jullien, F. Portier, P. Roche, A. Cavanna, Y. Jin, W. Wegscheider, P. Roulleau, and D. C. Glatli, Minimal-excitation states for electron quantum optics using levitons, *Nature (London)* **502**, 659 (2013).
- [12] T. Jullien, P. Roulleau, B. Roche, A. Cavanna, Y. Jin, and D. C. Glatli, Quantum tomography of an electron, *Nature (London)* **514**, 603 (2014).
- [13] L. S. Levitov, H. Lee, and G. Lesovik, Electron counting statistics and coherent states of electric current, *J. Math. Phys.* **37**, 4845 (1996).
- [14] D. A. Ivanov, H. W. Lee, and L. S. Levitov, Coherent states of alternating current, *Phys. Rev. B* **56**, 6839 (1997).
- [15] A. V. Lebedev, G. V. Lesovik, and G. Blatter, Generating spin-entangled electron pairs in normal conductors using voltage pulses, *Phys. Rev. B* **72**, 245314 (2005).
- [16] J. Keeling, I. Klich, and L. S. Levitov, Minimal Excitation States of Electrons in One-Dimensional Wires, *Phys. Rev. Lett.* **97**, 116403 (2006).
- [17] F. Hassler, M. V. Suslov, G. M. Graf, M. V. Lebedev, G. B. Lesovik, and G. Blatter, Wave-packet formalism of full counting statistics, *Phys. Rev. B* **78**, 165330 (2008).
- [18] J. Splettstoesser, M. Moskalets, and M. Büttiker, Two-Particle Nonlocal Aharonov-Bohm Effect from Two Single-Particle Emitters, *Phys. Rev. Lett.* **103**, 076804 (2009).
- [19] M. Moskalets and M. Büttiker, Spectroscopy of electron flows with single and two-particle emitters, *Phys. Rev. B* **83**, 035316 (2011).
- [20] F. D. Parmentier, E. Bocquillon, J.-M. Berroir, D. C. Glatli, B. Plaçais, G. Fève, M. Albert, C. Flindt, and M. Büttiker, Current noise spectrum of a single-particle emitter: Theory and experiment, *Phys. Rev. B* **85**, 165438 (2012).
- [21] E. Bocquillon, V. Freulon, J.-M. Berroir, P. Degiovanni, B. Plaçais, A. Cavanna, Y. Jin, and G. Fève, Coherence and Indistinguishability of Single Electrons Emitted by Independent Sources, *Science* **339**, 1054 (2013).
- [22] C. Grenier, R. Hervé, E. Bocquillon, F. D. Parmentier, B. Plaçais, J. M. Berroir, G. Fève, and P. Degiovanni, Single-electron quantum tomography in quantum Hall edge channels, *New J. Phys.* **13**, 093007 (2011).
- [23] D. Ferraro, A. Feller, A. Ghibaudo, E. Thibierge, E. Bocquillon, G. Fève, Ch. Grenier, and P. Degiovanni, Wigner function approach to single electron coherence in quantum Hall edge channels, *Phys. Rev. B* **88**, 205303 (2013).
- [24] J. Dubois, T. Jullien, C. Grenier, P. Degiovanni, P. Roulleau, and D. C. Glatli, Integer and fractional charge Lorentzian voltage pulses analyzed in the framework of photon-assisted shot noise, *Phys. Rev. B* **88**, 085301 (2013).
- [25] M. Moskalets, First-order correlation function of a stream of single-electron wave packets, *Phys. Rev. B* **91**, 195431 (2015).
- [26] B. Gaury and X. Waintal, Dynamical control of interference using voltage pulses in the quantum regime, *Nat. Commun.* **5**, 3844 (2014).
- [27] P. W. Anderson, Infrared Catastrophe in Fermi Gases with Local Scattering Potentials, *Phys. Rev. Lett.* **18**, 1049 (1967).
- [28] J. G. Proakis and M. Salehi, *Digital Communications*, 5th ed. (McGraw-Hill, New York, 2008).
- [29] I. Martin, G. Refael, and B. Halperin, Topological Frequency Conversion in Strongly Driven Quantum Systems, *Phys. Rev. X* **7**, 041008 (2017).
- [30] J. P. Dahlhaus, J. M. Edge, J. Tworzydło, and C. W. J. Beenakker, Quantum Hall effect in a one-dimensional dynamical system, *Phys. Rev. B* **84**, 115133 (2011).
- [31] I. Safi, Time-dependent transport in arbitrary extended driven tunnel junction, *arXiv:1401.5950*.
- [32] I. Safi and P. Joyez, Time-dependent theory of nonlinear response and current fluctuations, *Phys. Rev. B* **84**, 205129 (2011).
- [33] M. Moskalets and M. Büttiker, Floquet scattering theory of quantum pumps, *Phys. Rev. B* **66**, 205320 (2002).
- [34] G. B. Lesovik and L. S. Levitov, Noise in an ac Biased Junction: Nonstationary Aharonov-Bohm Effect, *Phys. Rev. Lett.* **72**, 538 (1994).
- [35] M. H. Pedersen and M. Büttiker, Scattering theory of photon-assisted electron transport, *Phys. Rev. B* **58**, 12993 (1998).
- [36] Th. Martin and R. Landauer, Wave-packet approach to noise in multichannel mesoscopic systems, *Phys. Rev. B* **45**, 1742 (1992).
- [37] M. Büttiker, Scattering theory of current and intensity noise correlations in conductors and wave guides, *Phys. Rev. B* **46**, 12485 (1992).
- [38] Ya. M. Blanter and M. Büttiker, Shot noise in mesoscopic conductors, *Phys. Rep.* **336**, 1 (2000).
- [39] V. S. Rychkov, M. L. Polianski, and M. Büttiker, Photon-assisted electron-hole shot noise in multiterminal conductors, *Phys. Rev. B* **72**, 155326 (2005).
- [40] M. Vanevic, Y. V. Nazarov, and W. Belzig, Elementary Events of Electron Transfer in a Voltage-Driven Quantum Point Contact, *Phys. Rev. Lett.* **99**, 076601 (2007).
- [41] D. Bagrets and F. Pistolesi, Frequency dispersion of photon-assisted shot noise in mesoscopic conductors, *Phys. Rev. B* **75**, 165315 (2007).

- [42] H. Fares, D. C. Glattli, Y. Louet, J. Palicot, P. Roulleau, and C. Moy, Power spectrum density of single side band CPM using Lorentzian frequency pulses, *IEEE Wireless Commun. Lett.* **6**, 786 (2017).
- [43] C. Grenier, R. Hervé, G. Fève, and P. Degiovanni, Electron quantum optics in quantum Hall edge channels, *Mod. Phys. Lett. B* **25**, 1053 (2011).
- [44] G. Haack, M. Moskalets, and M. Büttiker, Glauber coherence of single-electron sources, *Phys. Rev. B* **87**, 201302 (2013).
- [45] Yue Yin, On-demand electron source with tunable energy distribution, [arXiv:1709.08968](https://arxiv.org/abs/1709.08968).
- [46] Y. B. Sherkunov, A. Pratap, B. Muzykantskii, and N. d'Ambrumenil, Quantum point contacts, full counting statistics and the geometry of planes, *Opt. Spectrosc.* **108**, 466 (2010).
- [47] M. Knap, A. Shashi, Y. Nishida, A. Imambekov, D. A. Abanin, and E. Demler, Time-Dependent Impurity in Ultracold Fermions: Orthogonality Catastrophe and Beyond, *Phys. Rev. X* **2**, 041020 (2012).
- [48] P. P. Hofer and C. Flindt, Mach-Zehnder interferometry with periodic voltage pulses, *Phys. Rev. B* **90**, 235416 (2014).
- [49] M. Moskalets, Fractionally Charged Zero-Energy Single-Particle Excitations in a Driven Fermi Sea, *Phys. Rev. Lett.* **117**, 046801 (2016).
- [50] W. Belzig and M. Vanevic, Elementary Andreev processes in a driven superconductor-normal metal contact, *Phys. E (Amsterdam, Neth.)* **75**, 22 (2016).
- [51] R. H. Barker, Group Synchronizing of Binary Digital Systems, in *Communication Theory* (Butterworth, London, 1953), pp. 273–287.
- [52] D. C. Glattli and P. Roulleau, Hanbury-Brown Twiss noise correlation with time controlled quasi-particles in ballistic quantum conductors, *Phys. E (Amsterdam, Neth.)* **82**, 99 (2016).
- [53] J. Rech, D. Ferraro, T. Jonckheere, L. Vannucci, M. Sassetti, and T. Martin, Minimal Excitations in the Fractional Quantum Hall Regime, *Phys. Rev. Lett.* **118**, 076801 (2017).
- [54] M. Moskalets and G. Haack, Single-electron coherence: Finite temperature versus pure dephasing, in *Frontiers in Quantum Electronic Transport - in Memory of Markus Büttiker*, special issue of *Phys. E (Amsterdam, Neth.)* **75**, 358 (2016).
- [55] D. C. Glattli and P. Roulleau, Levitons for electron quantum optics, *Phys. Status Solidi B* **254**, 1600650 (2017).
- [56] F. Ronetti, L. Vannucci, D. Ferraro, T. Jonckheere, J. Rech, T. Martin, and M. Sassetti, Crystallization of levitons in the fractional quantum Hall regime, [arXiv:1712.07094](https://arxiv.org/abs/1712.07094).